Revista Brasileira de Geofísica
RBGf
Brazilian Journal of Geophysics

Revista Brasileira de Geofísica (2012) 30(1): 31-39

ISSN 0102-261X
www.scielo.br/rbg

PROPORTIONAL CONVOLUTION FILTERS – AN ALTERNATIVE TECHNIQUE FOR NON-DISTORTED IMAGE ENHANCEMENT

Fábio Cardinale Branco[1,2], Teodoro Isnard Ribeiro de Almeida[2] and Carlos Roberto de Souza Filho[3]

Recebido em 7 fevereiro, 2011 / Aceito em 8 maio, 2012
Received on February 7, 2011 / Accepted on May 8, 2012

ABSTRACT. This paper introduces a new class of spatial filters, here coined the proportional convolution filters. These filters are constructed in such way that the values assigned to each kernel cell are weighted as a function of the trigonometric distance of the cells to the kernel centre. A set of high-pass and low-pass proportional filters were designed using a specially tailored algorithm and a Delphi-based code that allows producing multi-dimensional filters. These filters underwent a twofold test. Firstly, the filters were tested against an instructive digital image of a candle flame. This image was employed as it shows large and detailed variations in color tones (low frequencies) and an assortment of possible boundaries between tones (high frequencies). Secondly, the filters were applied to a Landsat-5 TM image containing a variety of landforms. Results showed the efficiency of the filters and the adequacy of an array of kernel sizes to enhance both tonal and edge variations in a digital image, demonstrating that the proportional filters can benefit numerous applications in several fields of Geosciences.

Keywords: convolution filtering, high-pass, low-pass, image enhancement.

RESUMO. Este artigo apresenta uma nova classe de filtros espaciais, aqui denominados como filtros de convolução proporcionais. Esses filtros são construídos de tal forma que os valores atribuídos a cada célula do *kernel* são ponderados em função da distância trigonométrica das células para o centro do *kernel*. Um conjunto de filtros proporcionais, tanto passa-altas como passa-baixas, foi projetado usando um algoritmo especialmente adaptado e um código baseado em Delphi que permite a produção de filtros multidimensionais. Esses filtros foram submetidos a um teste duplo. Em primeiro lugar, os filtros foram testados em uma imagem digital de uma chama de vela. Esta imagem foi utilizada por mostrar grandes e progressivas variações de cor (baixas frequências) e uma variedade de possíveis limites entre os tons (frequências altas). Em segundo lugar, os filtros foram aplicados a uma imagem Landsat-5 TM com diversidade tonal e de formas de relevo. Os resultados mostraram a eficiência dos filtros e da adequação de diferentes tamanhos de *kernel* para melhorar tanto variações tonais como de borda em imagens digitais, demonstrando que os filtros proporcionais podem ter inúmeras aplicações em diversos campos das Geociências.

Palavras-chave: filtros de convolução, filtros passa-altas e passa-baixas, realce de imagens.

[1]EnvironMentality, Rua Michigan, 177 – Cidade Monções, 04566-000 São Paulo, SP, Brazil. Phone: +55 (11) 5561-3025; Fax: +55 (11) 5561-3025 – E-mail: fabio.tcl@uol.com.br

[2]Instituto de Geociências – USP, Rua do Lago, 562, Cidade Universitária, 05508-080 São Paulo, SP, Brazil. Phone: +55 (11) 3091-4236; Fax: +55 (11) 3091-4107 – E-mail: talmeida@usp.br

[3]Instituto de Geociências – UNICAMP, Rua Pandiá Calógeras, 51, Cidade Universitária Zeferino Vaz, Caixa Postal: 6152, 13083-970 Campinas, SP, Brazil. Phone: +55 (19) 3521-4535; Fax: +55 (19) 3521-4552 – E-mail: beto@ige.unicamp.br

INTRODUCTION

The spatial distribution of data in a digital image can be improved by a process known as spatial frequency filtering. This consists of using various mathematical transformations (Drury, 2001) to selectively emphasize or de-emphasize specific frequencies (high, medium or low) in the variation of the digital numbers (DNs) of the pixels of an image. Such mathematical filtering can be implemented in the spatial domain by a process known as convolution (Curran, 1985), which is used as one of the main filtering tools by image processing systems because it involves little computer time and simple mathematics, thus facilitating the use by beginners in image processing.

Convolution filtering has been applied in many areas, including noise filtering (Souza Filho et al., 1996), and the detection of edges and enhancement of specific variations in shades of grey (Mather, 1999), as well as the recognition of texture and shapes in remote sensing images (Blom & Daily, 1982), with special variations of filters developed for each of these applications (Holdermann et al., 1978; Drury, 2001).

Convolution filters are either high- or low-pass, i.e., they block all frequencies which are, respectively, lower or higher at a given cutoff frequency. By eliminating lower frequencies, the high-pass filter enhances edge and points, while excluding information about color variation. Moreover, the enhancement of lines can be spatially controlled to emphasize all lines in a given direction. Usually, however, such directional control is not relevant, and non-directional convolution filters are preferable.

In developing non-directional, isotropic convolution filters, two main issues must be addressed: 1) the kernel dimensions (number of cells in the matrix) of the convolution filter and 2) the weight attributed to each of these cells. The dimensions of the filter determine the extent to which an image will be altered, with the choice being a function of the scale of the features to be enhanced, smoothed, or concealed. With low-pass filters, a small matrix will eliminate very little information, while larger ones result in the enhancement of larger features, although eliminating finer ones. With high-pass filters, however, smaller matrices result in the elimination of more information, providing finer spacing or better definition of finer edges. A high-pass filter normally enhances features that are less than half the size of the convolution matrix used (Drury, 2001).

As stated by Drury (2001), along the convolution operation "...*a matrix is overlain on the image with its central cell on top of a pixel and the other cells lying on top of the immediately surrounding pixels. The DN for each pixel overlain by the convolution matrix is multiplied by the corresponding weighting factor and the products are summed. It is this sum of local area operations that is used to compute the value to be used in place of the DN of the pixel beneath the centre of the convolution matrix. An output image is produced by the convolution matrix systematically being moved over and transforming the DN of every pixel in the image*..." Although this notion on spatial filtering is widely acknowledged, a technique that can efficiently balance the distribution of weights in a kernel tailored for geological and geobotanical applications has not been proposed yet.

Weight distribution involves tradeoffs favoring those pixels located closer to the central cell of the matrix, since these are generally more highly correlated with the central pixel than to more distant ones. In this way, the distortion inherent in the process of convolution filtering is reduced, although a certain amount will always exist, since the weights are distributed in a discrete rather than a continuous manner in the kernel (Branco, 1998).

In this paper, a new approach for calculating these weights is proposed. It is based on the trigonometric distance of each cell from the central cell. A program in Delphi code was developed for the generation of these filters, henceforth denominated proportional convolution filters (PCFs). The low- and high-pass PCFs were tested on two types of images: a very simple image of a candle flame and a Landsat-5 TM image. The latter was aimed to demonstrate the validity of the proposed method as a technique for the digital processing of remote sensing data.

METHODOLOGY

Basis and development of proportional convolution filters

Analysis of the various convolution filters described in the literature shows a tendency to attribute greater weight to more central matrix cells, based on the principle that the distribution of weights should be inversely proportional to the distance of each cell from the central one, thus honoring the geometry of the features present in the original image.

An image can be represented by the function $P_{i,j}$ for the original DN of each pixel in the image matrix, where i and j are the row and column coordinates of that pixel. The filter used is a box filter, which consists of a matrix of dimensions $2M + 1$ rows by $2N + 1$ columns to guarantee that the number of rows and cells is always odd so that a single cell will always be at the exact center of the matrix. Each cell in this box filter has a weighting of C, so the complete matrix can be expressed by the function $C_{k,l}$, with k and l being the cell coordinates within the filter.

The calculation involved in a PCF is shown below for both high- and low-pass versions. A high-pass PCF is yielded through the following equation:

$$D_{k,l} = \sqrt{k^2 + l^2} \tag{1}$$

where:

$D_{k,l}$ = distance of cell $C_{k,l}$ from the center cell;
k = column indicator;
l = line indicator.

For a high-pass PCF, the value of each cell (except the central one) must be negative and inversely proportional to its distance from the center cell of the filter. The calculation of all cells in the filter but the central cell is possible through the equation given below:

$$C_{k,l} = \frac{-1}{D_{k,l}} = \frac{-1}{\sqrt{k^2 + l^2}} \tag{2}$$

The calculation of the central cell is accomplished by summing the absolute values of all the other cells:

$$C'_{k,l} = \sum_{k=-M}^{k=+M} \sum_{l=-N}^{l=+N} \frac{1}{\sqrt{k^2 + l^2}} \tag{3}$$

For a low-pass PCF, the calculation of all cells is similar, except that all their values are positive and given by:

$$C_{k,l} = \frac{1}{D_{k,l}} = \frac{1}{\sqrt{k^2 + l^2}} \tag{4}$$

The central cell of a low-pass filter, however, is given a value of 1, since the function of such filtering is to exclude punctual high-frequency information and favor that with greater spatial expression. In other words, the original pixel will be replaced by the average of the values of the neighboring cells, thus "regionalizing" the information.

The convolution operation of a box filter on an image $P_{i,j}$ to produce a new image $O_{i,j}$ is expressed as in the equation below (Drury, 2001):

$$O(i, j) = \sum_{k=-M}^{M} \sum_{l=-N}^{N} \times P(i + k, j + l)^* C(k + M + 1, l + N + 1) \tag{5}$$

This equation can be modified for a high-pass PCF by means of Equation 6, which involves the combination of Equations 2 and 3 with Equation 5.

$$\begin{aligned} O_{i,j} = & \left[\sum_{k=1}^{k=M} \sum_{l=-N}^{l=N} -\frac{P_{(i+k,j+l)}}{\sqrt{k^2 + l^2}} \right] \\ & + \left[\sum_{k=-M}^{k=-1} \sum_{l=-N}^{l=N} -\frac{P_{(i+k,j+l)}}{\sqrt{k^2 + l^2}} \right] \\ & + \frac{P_{i,j}}{\sum_{k=-M}^{k=M} \sum_{l=-N}^{l=N} \sqrt{k^2 + l^2}} \end{aligned} \tag{6}$$

For low-pass PCFs, the kernel is obtained by the inclusion of Equation 4 in Equation 5, which gives the following:

$$\begin{aligned} O_{i,j} = & \left[\sum_{k=1}^{k=M} \sum_{l=-N}^{l=N} -\frac{P_{(i+k,j+l)}}{\sqrt{k^2 + l^2}} \right] \\ & + \left[\sum_{k=-M}^{k=-1} \sum_{l=-N}^{l=N} -\frac{P_{(i+k,j+l)}}{\sqrt{k^2 + l^2}} \right] + P_{i,j} \end{aligned} \tag{7}$$

In order to facilitate the generation of PCFs and their application in image processing routines, a program in Delphi was produced to automatically create multi-dimensional high- and low-pass PCFs in a format accepted by numerous open and commercial software packages. This program is provided as part of the manuscript and a general view of its operational window is illustrated and commented in the Appendix.

Figure 1 shows the geometry of the northeast quadrant of the high-pass and low-pass PCFs with 13 × 13 cells, where the radial contours indicate the distance of the cells from the center of the filter.

The PCFs are conceptually similar to Gaussian convolution filters (e.g., Tao & Asari, 2004 and references therein) but show enhanced features. Most importantly, the PCFs have the advantage to produce cell weights lineally proportional to the distance from the central cell. This avoids that cells distant from the center are assigned with null values independently of the dimensions of the kernel – a feature particularly important in large kernels that is not taken in account in Gaussian filters.

Evaluation of the PCFs

Three basic approaches were used for the analysis of the proposed PCFs:

(i) a first approach assumes the traditional exclusion of grey tones (low frequencies) and edges (high frequencies) through high-pass and low-pass PCFs, respectively. If the

-0.167	-0.164	-0.158	-0.149	-0.139	-0.128	-0.118
-0.200	-0.196	-0.186	-0.171	-0.156	-0.141	-0.128
-0.250	-0.243	-0.224	-0.200	-0.177	-0.156	-0.139
-0.333	-0.316	-0.277	-0.236	-0.200	-0.171	-0.149
-0.500	-0.447	-0.354	-0.277	-0.224	-0.186	-0.158
-1.000	-0.707	-0.447	-0.316	-0.243	-0.196	-0.164
≥41.96	-1.000	-0.500	-0.333	-0.250	-0.200	-0.167

0.167	0.164	0.158	0.149	0.139	0.128	0.118
0.200	0.196	0.186	0.171	0.156	0.141	0.128
0.250	0.243	0.224	0.200	0.177	0.156	0.139
0.333	0.316	0.277	0.236	0.200	0.171	0.149
0.500	0.447	0.354	0.277	0.224	0.186	0.158
1.000	0.707	0.447	0.316	0.243	0.196	0.164
1	1.000	0.500	0.333	0.250	0.200	0.167

Figure 1 – A: 'Geometry' of a 13 $\times$ 13 high-pass proportional convolution filter (only NE quadrant of the kernel is shown). B: 'Geometry' of a 13 $\times$ 13 low-pass proportional convolution filter (only NE quadrant of the kernel is shown). Arcs are explicatory isovalues.

application of these two PCFs does not cause distortion, it should be possible to obtain a new image, equivalent to the original one, by the sum of the images filtered by high- and low-pass PCFs with the same dimensions. This test was conducted on a 350 $\times$ 350 pixel segment of a Landsat-5 TM band 4 (TM4) image using filters of 31 $\times$ 31 cells and 127 $\times$ 127 cells.

(ii) a full correlation between the original image and the sum of the filtered images is not a complete proof of the lack of distortions; since such effects could be inversely complementary and compensated by both high- and low-pass filters. Thus, in a second approach to prove that no distortions are generated through PCF processing, we measured the numeric correlations in a series of PCFs with different dimensions. To test high-pass PCFs, we applied 28 filters, with dimensions varying between 3 $\times$ 3 and 255 $\times$ 255 cells, over a segment of the TM4 image. The degree of correlation between the filtered images and the original TM4 image should increase as the dimension of the filters escalate. When the filter dimensions surpass the original image in size, however, all features are of high-frequency, and the filtered image will be identical to the original (no information will be considered to be of low-frequency). It is important to highlight that in convolution filtering such test must take in account that the information from some of the external rows and columns is lost due to the boundary effect. Nonetheless, the correlation curve is likely to display a coherent tendency.

(iii) a third approach involves a simple image of a candle flame, since the internal portion of the flame is known to reveal temperature variations, and consequently, a very interesting gradient of colors. Assuming that a low-pass filter will enhance information about color, these variations should be much clearer in the filtered image than in the original one. By varying the dimensions of the filter, it should be possible to relate filter dimensions to feature characteristics. The candle flame was photographed with ASA 100 Fujicolor film, with diffuse RMS granularity (SD of 9), which has a resolution of 100 pairs of lines per millimeter, in contrast to the 1000 to 1 in standard development. The photograph obtained was digitalized in a scanner with a resolution of 400 dpi in 3 channels (red, green and blue) of 8 bits each, resulting in a jpeg-format image. For this test, low-pass PCFs were employed with four different dimensions: 45 $\times$ 45, 65 $\times$ 65, 101 $\times$ 101, and 201 $\times$ 201 cells. This variation was considered sufficient to illustrate the effects of filters of different dimensions. Since the purpose was to compare the effects of the filter in the color composition, each filter was applied to the red, green and blue channels. After the application of the filters, the grey levels were stretched to occupy the 0-255 range, using a histogram equalization function. The same experiment was repeated with high-pass PCFs, although filters with smaller dimensions were used (7 $\times$ 7, 15 $\times$ 15, 31 $\times$ 31 and 61 $\times$ 61 cells).

RESULTS AND DISCUSSION

(i) in the first quantitative test, the sum of the images yielded through low-pass and high-pass PCFs revealed 100% correlation with the original image.

(ii) the application of 28 filters with varied dimensions confirms these results, with an increase of correlation occurring in agreement with an increase of high-pass PCFs dimensions, as expected (Fig. 2). For low-pass PCFs, the correlation curve is equivalent (not shown), since the excluded information by high-pass filters is maintained by a low-pass filter, and the correlation between a remote sensing image using proportional low-pass filters and the original image tends to decrease with an increase in filter dimensions. In numerical terms, the correlation of the original image to that filtered by a 31 $\times$ 31-kernel and by a 255 $\times$ 255-kernel is 63.6% and 40.9%, respectively. This analysis, however, varies with the nature of the original data. The rougher the texture of the original image, the lower it will be the correlation between the filtered image and the original, as long as the same filter size is used.

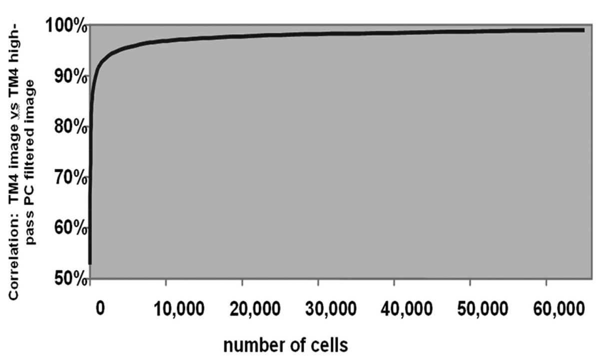

Figure 2 – Diagram showing the correlation between the original TM4 image and the resulting high-pass PC filtered TM4 image (Y-axis) *vs.* the number of cells employed in the high-pass PCF (X-axis).

Figure 3 display a segment of a Landsat image (band 4) including the area around the Camaquã copper mines, located in the Rio Grande do Sul State, southern Brazil. Following the notions above mentioned, it is possible to observe that a large part of the tonal information in image 3A, which enables the distinction of photogeological units, was lost after a high-pass PCF was applied (Fig. 3B). However, the textural information in 3A was enhanced in 3B, which shows, for example, a marked radial drainage pattern less visible in the non-filtered image. Image 3C, in contrast, contains only the tonal information, which was lost with high-pass filtering.

Figure 4 shows DN profiles extracted from the original TM band 4 image and equivalent 31 $\times$ 31 cells and 101 $\times$ 101 cells low-pass filtered images. The filtered images show a great reduction in high-frequency features, whereas the lower frequency features are strongly enhanced, thus indicating that there was no significant distortions due to the filtering process. In the original image, the low-frequency information is difficult to distinguish, although it is clear in the filtered image, since it has been enhanced.

(iii) Figure 5 shows the results of low-pass PC filtering of a flame image. Several filter dimensions were employed, spanning from 45 $\times$ 45, 65 $\times$ 65, 101 $\times$ 101 and 201 $\times$ 201 cells. A qualitative assessment of the pictures shows that the base of the flame portrays a gradation of colors from black to white, including various tones of red and yellow. A comparison of the original image (Fig. 5A) with those in 5B and 5C shows that the color intensity in the filtered images is greater, which indicates the intended enhancement. Likewise, the yellow central portion of the flame, faint in the Figure 5A image and enhanced in Figures 5B and 5C, is fuzzier in Figure 5D. Figure 5E shows the internal features and the visible external contour of the flame, but significantly distorted. This distortion is the result of the excessively large dimensions of the filter, which thus includes uncorrelated background pixels in the convolution. This is especially clear in the contour of the lower portion of the flame, initially concave, but convex after filtering. Similarly, the enlargement of the top of the flame in Figures 5G, 5H and 5I clearly shows various colored regions, although their definition are not clear in the original image (5F). Image 5J shows the presence of important artifacts, again due the excessive filter size.

The effect of high-pass PCFs applied to original flame image of Figure 5A is seen in Figure 6, which shows the results yielded by filters with dimensions of 7 $\times$ 7, 15 $\times$ 15, 31 $\times$ 31 and 61 $\times$ 61 cells (Figs. A, B, C, and D, respectively). Here, the edge of the flame is sharply defined in all four images, but its thickness varies in relation to the filter used. The information about the original color in the interior of the flame is lost when a smaller number of cells are included in the high-pass filter (Figs. 6A and 6B). Given the image resolution and the filter dimensions tested, it is clear that this information is related to low frequencies of color variation. When larger filters are employed, color features at the base of the flame appear as in image 6C, and are even more obvious in Figure 6D. This effect of kernel size is explained in Figure 2. The original color information disappears with the use of smaller high-pass filters (Figs. 6A and 6B), since for filter dimensions between 7 $\times$ 7 and 15 $\times$ 15 cells, this class

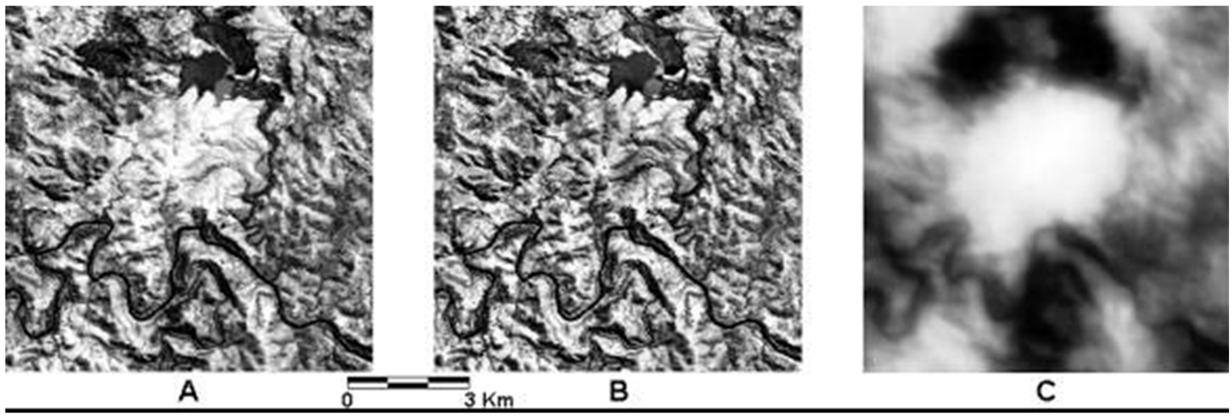

Figure 3 – Landsat image of the area around the Camaquã copper mines, located in the Rio Grande do Sul State, southern Brazil. Original (unfiltered) TM band 4 image (A). TM band 4 convolved by 77 $\times$ 77 high-pass (B) and low-pass (C) proportional convolution filters, respectively.

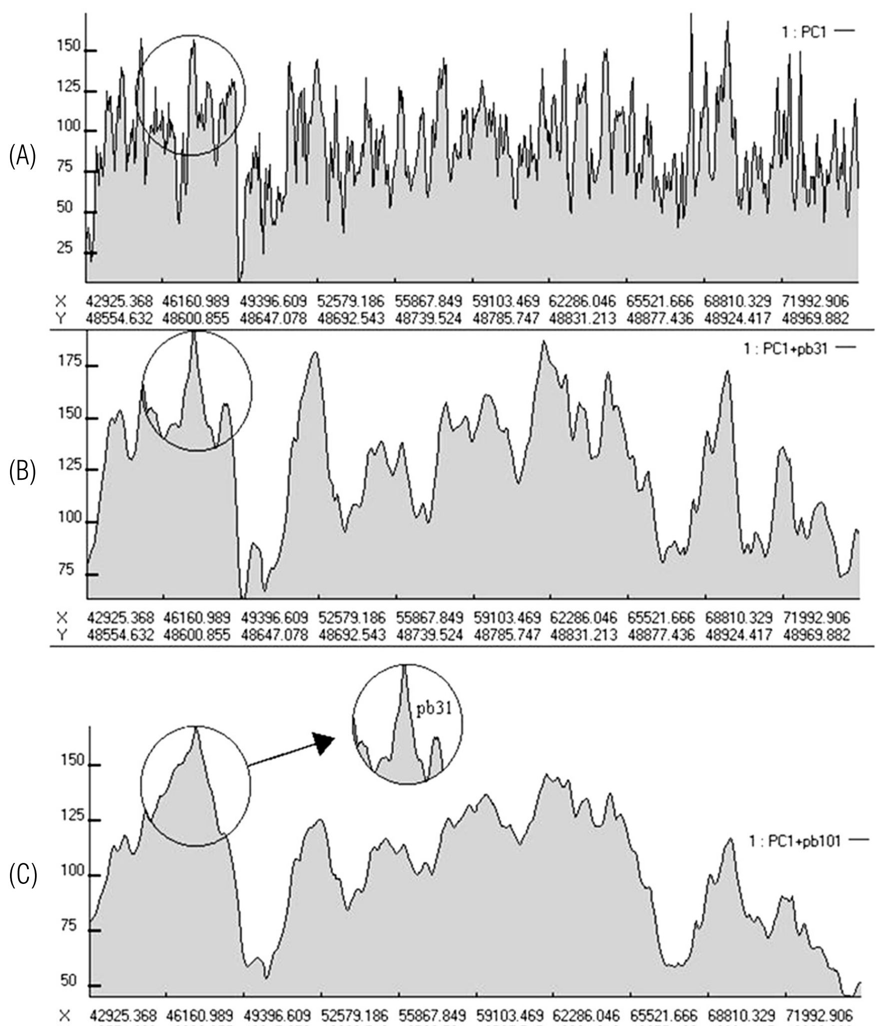

Figure 4 – DN profiles extracted from the TM band 4 image. Original image (A). TM4 convolved by 31 $\times$ 31 (B) and 101 $\times$ 101 (C) low-pass proportional convolution filters. For comparison, the circles indicate the same region at the three profiles. X and Y coordinates of the samples are given at the bottom of each profile.

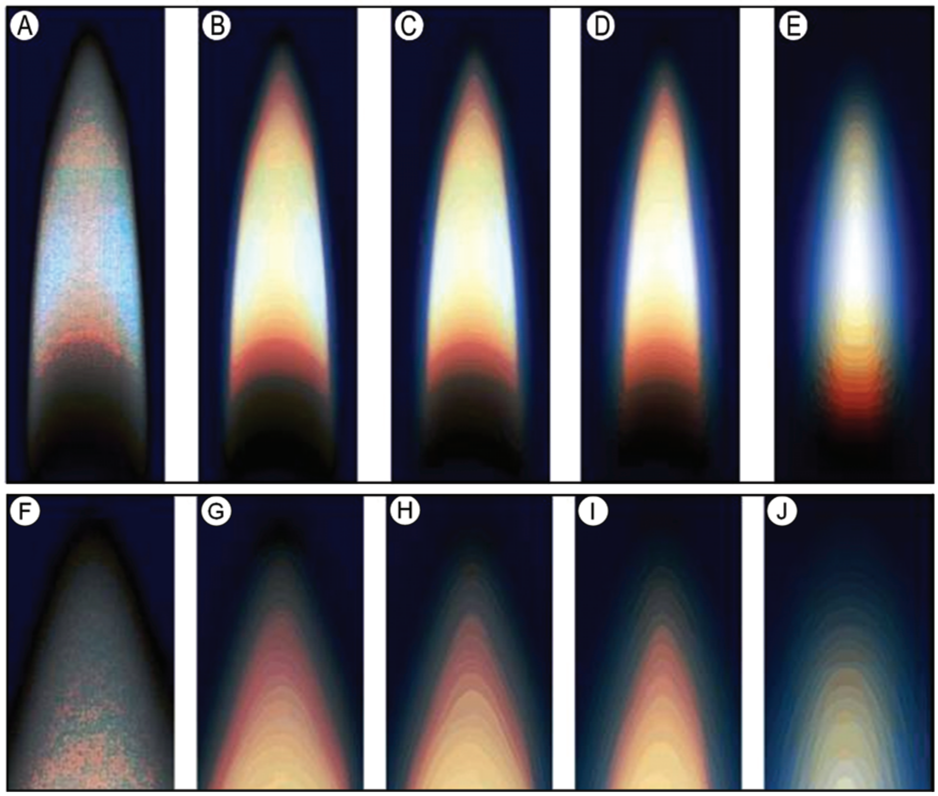

Figure 5 – (A) Raw candle flame image. Figures (B) to (E) are low-pass PC filtered images with kernels made of 45 × 45, 65 × 65, 101 × 101 and 201 × 201 cells. Figures (F) to (J) are respective enlargements of the top of the flame. The images were contrast enhanced using an equalization function.

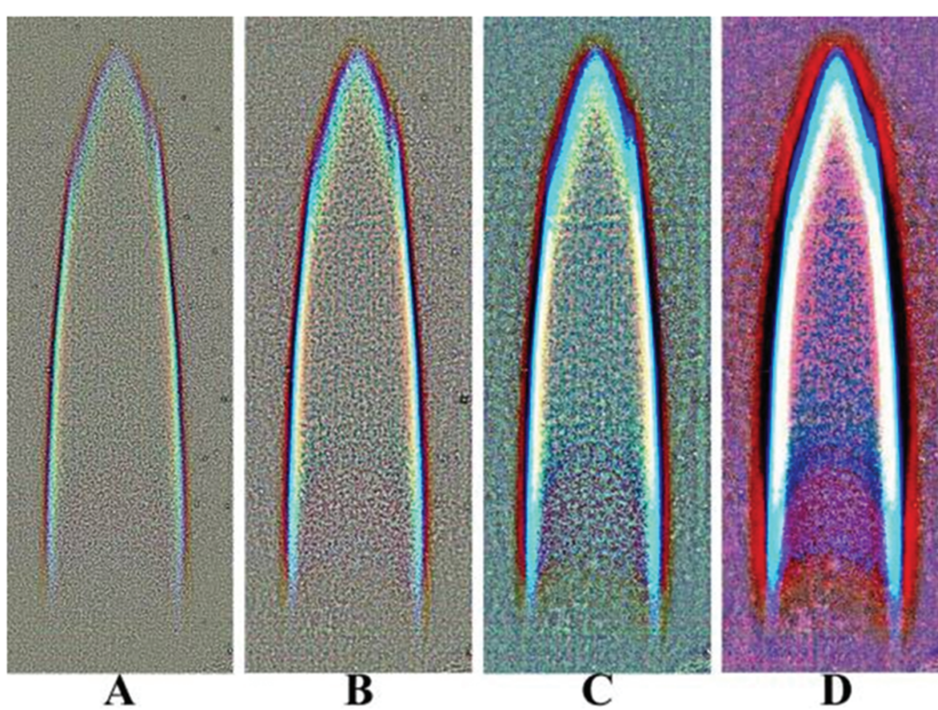

Figure 6 – Images of a candle flame after high-pass proportional convolution filtering. Figures (A) to (D) were produced with kernels made of 7 × 7, 15 × 15, 31 × 31 and 61 × 61 cells, respectively.

of information is related to low frequencies in a tone variation. When larger filters are applied (Figs. 6C and 6D), the spectral information referring to the different color features present at the base of the flame starts to appear in the image (Fig. 6C, 31 × 31 filter), and is clearly visible in Figure 6D (61 × 61 filter). This image shows visually that with the increase in filter size the correlation with the original image increases, since the number of features considered to be of high-frequency in the filtering process also increases.

CONCLUSIONS

The method proposed in this paper for the construction a new class of filter – the proportional convolution filter – has proved successful for the establishment of adequate box sizes for filters used to enhance remote sensing images. The use of low-pass PCFs makes it possible to enhance spectral, tonal information, although information contained in a texturally rich image must be added back to the low-pass filtered product for throughout image interpretation. This procedure facilitates the interpretation of an image by furnishing both textural and edge information. Moreover, filter dimensions are critical. When adequately selected in relation to feature size (in terms of number of pixels), the resulting image shows no significant distortions. Furthermore, filters larger than those usually found in the literature will often by necessary. In the production of such large filters, however, it is extremely important to use weights proportional to the distance from the center in order to achieve distortion-free results.

ACKNOWLEDGMENTS

The authors thank Mr. Antonio Tadashi Kikuda for his assistance with the Delphi code and FAPESP (Fundação de Amparo à Pesquisa do Estado de São Paulo) for funding the project (Proc. N. 96/03347-4). C.R. Souza Filho acknowledges CNPq for the Research Grant (No. 301.227/94).

APPENDIX

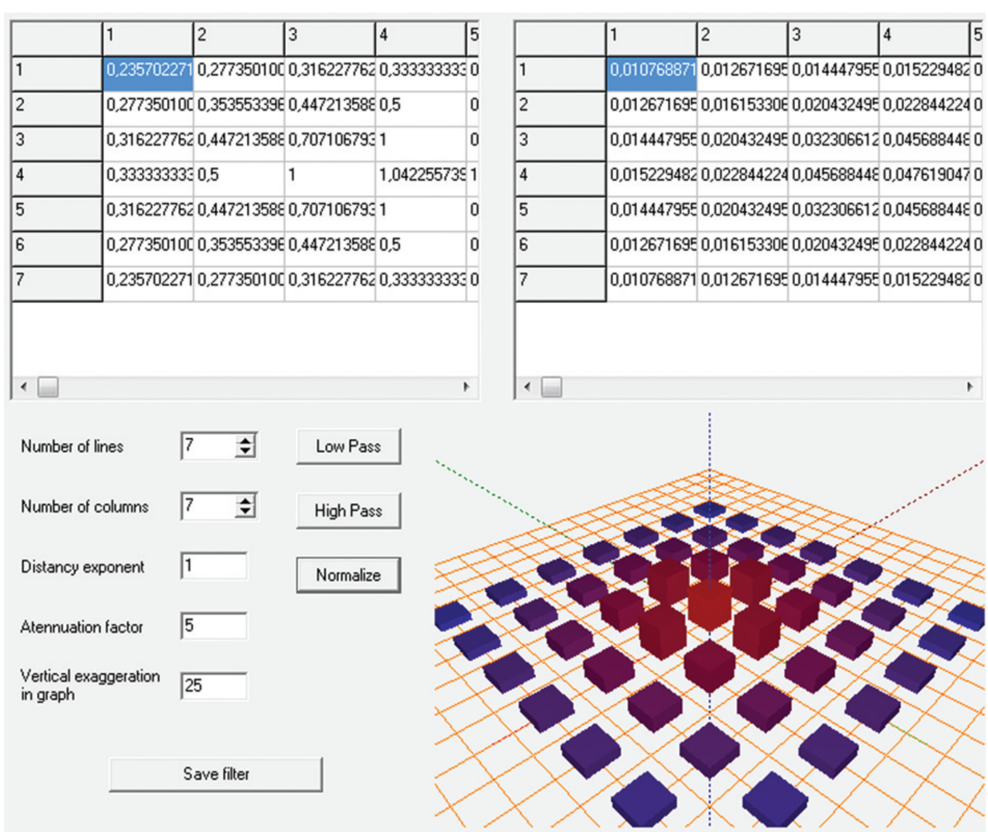

Appendix – Illustration of the proportional convolution filter (PCF) software interface. In order to run the program and create a spatial filter, the user must provide the number of lines and columns to be used in the kernel and to specify whether it will be a low-pass or a high-pass filter. The user can also favor a high or low gradient between adjacent values in the kernel by playing with the distance exponent option (default value is 1) and the attenuation factor (default value is 0). To graphically preview the distribution of relative weights in the kernel, it is possible to visualize it as a grid of blocks with varying vertical exaggerations (default value is 10).

REFERENCES

BLOM RG & DAILY M. 1982. Radar Image-Processing for Rock-Type Discrimination. IEEE Transactions on Geoscience and Remote Sensing, 20(3): 343–351.

BRANCO FC. 1998. Filtros de Convolução Passa Baixas no Realce Tonal de Imagens. M.Sc. Dissertation. Instituto de Geociências – USP. São Paulo, SP, Brazil, 78 pp.

CURRAN PJ. 1985. Principles of Remote Sensing. Longman Group Limited, London, UK, 282 pp.

DRURY SA. 2001. Image Interpretation in Geology. Blackwell Science, UK, 3rd edition, 296 pp.

HOLDERMANN F, BOHNER M, BARGEL B & KAZMIERCZAK H. 1978. Review of Automatic Image Processing. Photogrammetria, 34: 225–258.

MATHER PM. 1999. Computer Processing of Remotely-Sensed Images: An Introduction. John Wiley & Sons Inc., UK, 292 pp.

SOUZA FILHO CR, DRURY SA, DENNISS AM, CARLTON RWT & ROTHERY DA. 1996. Restoration of Corrupted Optical Fuyo-1 (JERS-1) Data Using Frequency Domain Techniques. Photogrammetric Engineering & Remote Sensing, 62(9): 1037–1047.

TAO L & ASARI V. 2004. An Integrated Neighborhood Dependent Approach for Nonlinear Enhancement of Color Images. In: International Conference on Information Technology, Proceedings. 2: 138–139.

NOTES ABOUT THE AUTHORS

Fábio Cardinale Branco has a B.Sc. degree in Geology (Universidade de São Paulo, 1992), and a M.Sc. in Geology at Hydrogeology and Mineral Resources Graduate Program (Universidade de São Paulo, 1998). Since 1996 he is working as a consultant in air pollution and environmental impacts of vehicle emissions.

Teodoro Isnard Ribeiro de Almeida has a B.Sc. degree in Geology (Universidade de São Paulo, 1977), a M.Sc. in Remote Sensing (Instituto Nacional de Pesquisas Espaciais – INPE, 1982) and a Ph.D. in Geology (Universidade de São Paulo, 1991). In 1999, carried out research on Geobotany as part of a postdoctoral fellowship at the Toulouse University (France). Since 1990 he is working as an Associate Professor and Senior Researcher at the Universidade de São Paulo, where he has also been the Coordinator of the Geosciences Graduate Research Program in Hydrogeology and Mineral Resources between 2003 and 2012. He is a Level 2 Researcher at the Conselho Nacional de Desenvolvimento Científico e Tecnológico (CNPq).

Carlos Roberto de Souza Filho graduated on Geological Engineer (Universidade Federal de Ouro Preto, 1988). He holds a Master degree in Metalogenesis (Universidade Estadual de Campinas – UNICAMP, 1991) and a Ph.D. on Earth Sciences/Remote Sensing (The Open University, England, 1995). At UNICAMP, became an Assistant Professor in 1997, an Associate Professor in 2002 and achieved the Full-Professorship in 2008. He is currently the General Coordinator of the Graduate Research Programs at the Geosciences Institute and the leader of the Research Team on Geotechnologies. He is a Level 1A Researcher at the Conselho Nacional de Desenvolvimento Científico e Tecnológico (CNPq) and Member of the São Paulo Academy of Sciences. He is responsible for several scientific laboratories, including the Reflectance Spectroscopy lab, the FTIR spectroscopy lab and a suite of Image Processing labs at UNICAMP.